WANL-TME-1558

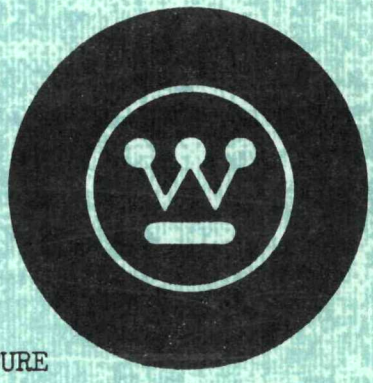

Westinghouse Astronuclear Laboratory

A STUDY OF VARIOUS HEATING METHODS FOR HIGH TEMPERATURE TESTING OF FUEL ELEMENTS

(Title Unclassified)

CONFIDENTIAL
RESTRICTED DATA
Atomic Energy Act - 1954

RECORD COPY

DISCLAIMER

[redacted] Act - 195[redacted]

Astronuclear Laboratory

WANL-TME-1558

[redacted]

40

A STUDY OF VARIOUS HEATING METHODS FOR HIGH TEMPERATURE TESTING OF FUEL ELEMENTS

(Title Unclassified)

by

J. W. H. Chi
and
R. L. Ramp
Thermo-Flow Laboratory

Approved:

W. J. Havener

W. J. Havener, Manager
High Power Programs

[redacted] - 1954

[redacted] 1954

Astronuclear Laboratory

WANL-TME-1558

ABSTRACT

NERVA fuel elements have been and are being tested in high temperature furnaces by resistance (or ohmic) heating of the fuel elements. Although the axial temperature distribution obtained simulates fairly closely that of the reactor, the cross-sectional temperature distributions are known to be different. This difference has been suspected to be a prime source of difficulty in obtaining a significant correlation between the corrosion performance of furnace-tested elements and that of reactor-tested fuel elements. As a consequence, other types of furnace heating methods have been suggested. Several possible methods are studied in this memorandum. The effect of various modes of heating on the cross-sectional temperature distributions were analyzed with the aid of a TOSS model. The advantages and disadvantages of the various methods are discussed.

It was concluded that both induction and radiation heating are unsatisfactory and impractical. Passive heating is useful for the study of local conditions only, but the cross-sectional temperature gradients are in reverse to those observed in the ohmic heated elements. In-pile heating is obviously the ideal method. However, the high cost of testing and the slow turn-around time precludes a serious consideration of this method. It was concluded that ohmic heating is still the most practical method for large-scale testing of fuel elements.

[redacted] 1954

INTRODUCTION

The object of development and qualification testing of NERVA fuel elements is to determine the behavior of the elements under conditions as closely simulating actual reactor operation as possible. These conditions include relatively uniform power generation throughout the cross-section of the fuel element and a predetermined power input. The heat generated in the fuel element is transferred to the gaseous hydrogen flowing through the fuel element coolant channels at a given flow rate and pressure drop. The pressure and flow of the hydrogen through the heated element can be accurately simulated. However, the method of heat generation in the element and its effect on the temperature distribution in the fuel element has been of some concern. Recently, it has been suggested that induction heating be investigated.

This memorandum presents a study of the various methods of heating and an analysis of their effects on the temperature distribution in the fuel element. The various possible methods of heating are:

1. Resistance Heating
2. Induction Heating, and
3. Radiation Heating

Electrical resistance or ohmic heating is the method currently used in the fuel element test program. In all of these methods, it is possible to attain identical axial temperature profiles similar to that in the reactor by controlling the total heat input and the hydrogen flow rate. The primary difference arises

in the cross-sectional temperature distributions and the temperature gradients, which should be minimized; consequently, a comparison of the various heating methods reduces to a comparison of the cross-sectional temperature distributions. For this purpose, a TOSS model was used and the results are discussed in this memorandum. Particular emphasis is placed on induction heating, as it had been suggested as a possible alternative to ohmic heating.

RESISTANCE HEATING

In the present method of heating an element in a corrosion test, a d.c. power supply with variable voltage is connected to each end of the element with graphite chucks. The voltage is adjusted to approximately 200 volts, and for a typical element, the resulting current and power are 4000 amperes and 800 kilowatts. Concentric molybdenum heat shields around the element reduce the radiation heat loss to approximately 7%.

The fuel element chucks and heat shields are enclosed in a water-cooled pressure vessel filled with helium. With direct current, or ohmic heating, the heat generation rate throughout the element is the same. The flow rate, inlet temperature, and pressure of the hydrogen gas and the radiation and conductive heat losses determine the temperature profile along the axial length of the fuel element. The cross-sectional temperature distribution of the fuel element with resistance heating shall be used as the reference case with which the other cases will be compared.

Cross-sectional Temperature Distribution

An analysis of the cross-sectional temperature distribution was carried out with a two-dimensional TOSS model. Details on the TOSS model are presented in the appendix. Two cases were investigated; one in which heat generation in the NbC liners was not considered and one in which heat generation in the NbC liners was accounted for. Heretofore, the occurrence of cracks in the NbC liners

permitted the assumption that heat is not generated in the liners. However, the presence of special overcoats may effectively bridge the crack gaps, thereby providing continuous current paths through the liners. The thickness of the NbC liners was assumed to be 2 mils. The results from an analysis of the two cases are presented in Figures 1 and 2 and compared in Figure 3. Figure 1 is a map of the temperature distributions when heat generation in the NbC liners is neglected. Figure 2 is a similar plot for the case where heat generation in the NbC liners is included. Figure 3 is a plot of the maximum and minimum radial temperature gradients versus the distance normal to the surface of the coolant channels. In both cases, the maximum temperature gradients occurred near the central coolant channel, while the minimum temperature gradients were found near the element surface as shown on the inserted sketch of the fuel element model. It is important to note that the differences in temperature gradients between the maximum and minimum curves are significantly greater than the differences in temperature gradients with and without heat generation in the NbC coatings. On the basis of this analysis, it may be concluded that no significant changes in thermal stresses are anticipated when heat generation in the NbC coatings occur.

It should be pointed out that the temperatures shown in the figure represent those occurring at a station of 50 In.* with a total power generation of 850 KW and a hydrogen flowrate of 500 Scfm. For a more complete analysis of temperature distributions with resistance heating, see references 1 and 2.

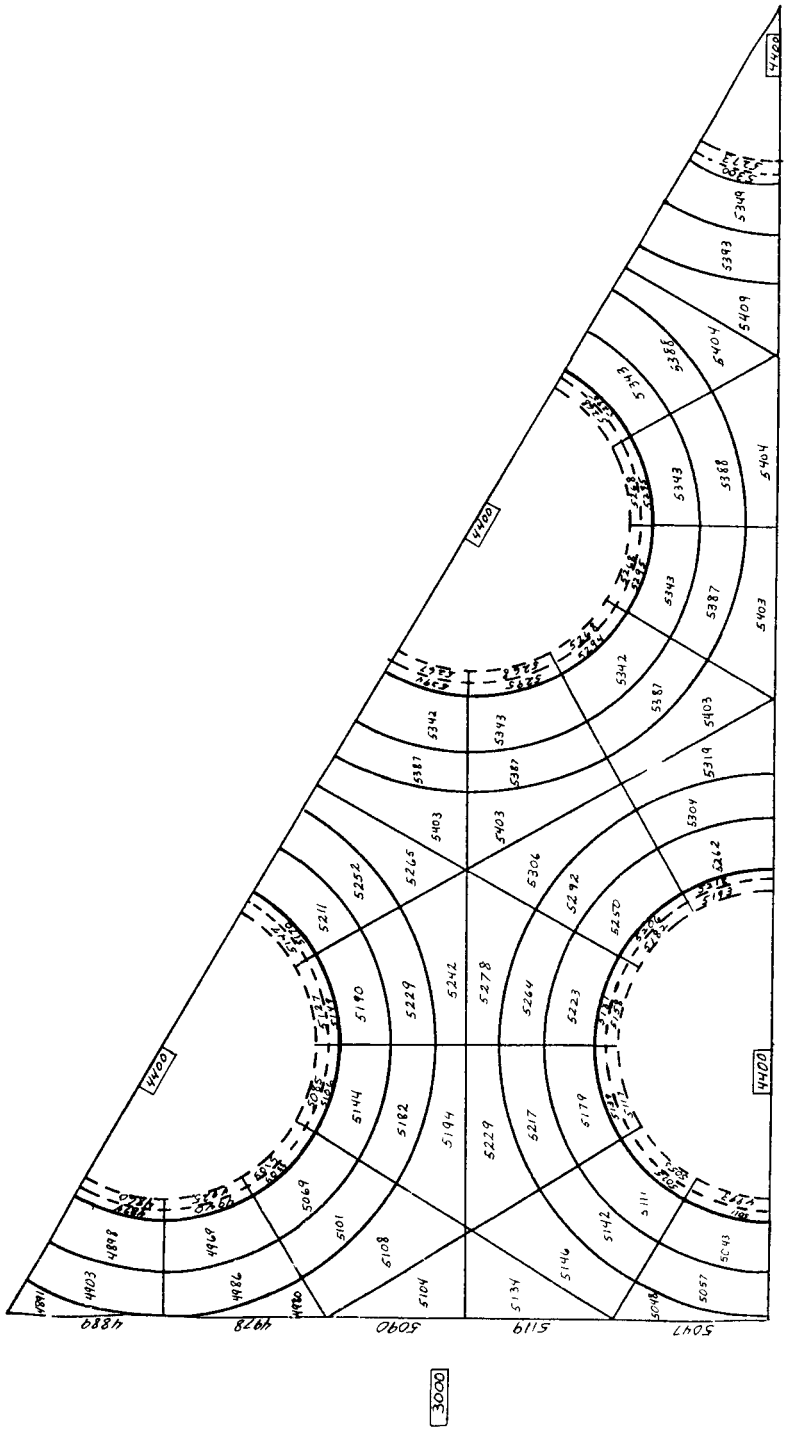

Figure 1

Temperature Distribution with Heat Generation
In the NbC Neglected; 850 KW
Total Power; Temperature In °R

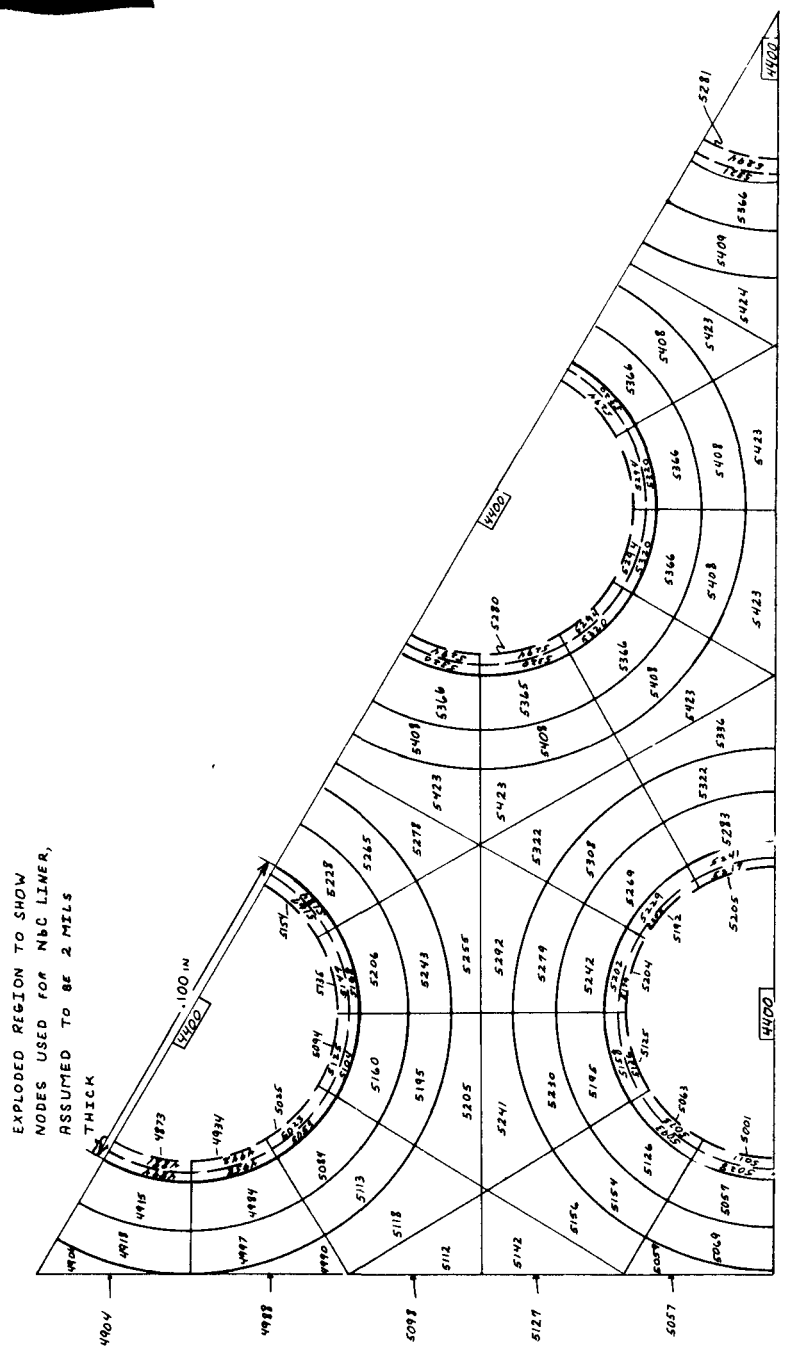

Figure 2

Temperature Distribution with Heat Generation in the NbC Taken into Consideration; 850 KW Total Power; Temperatures in °R

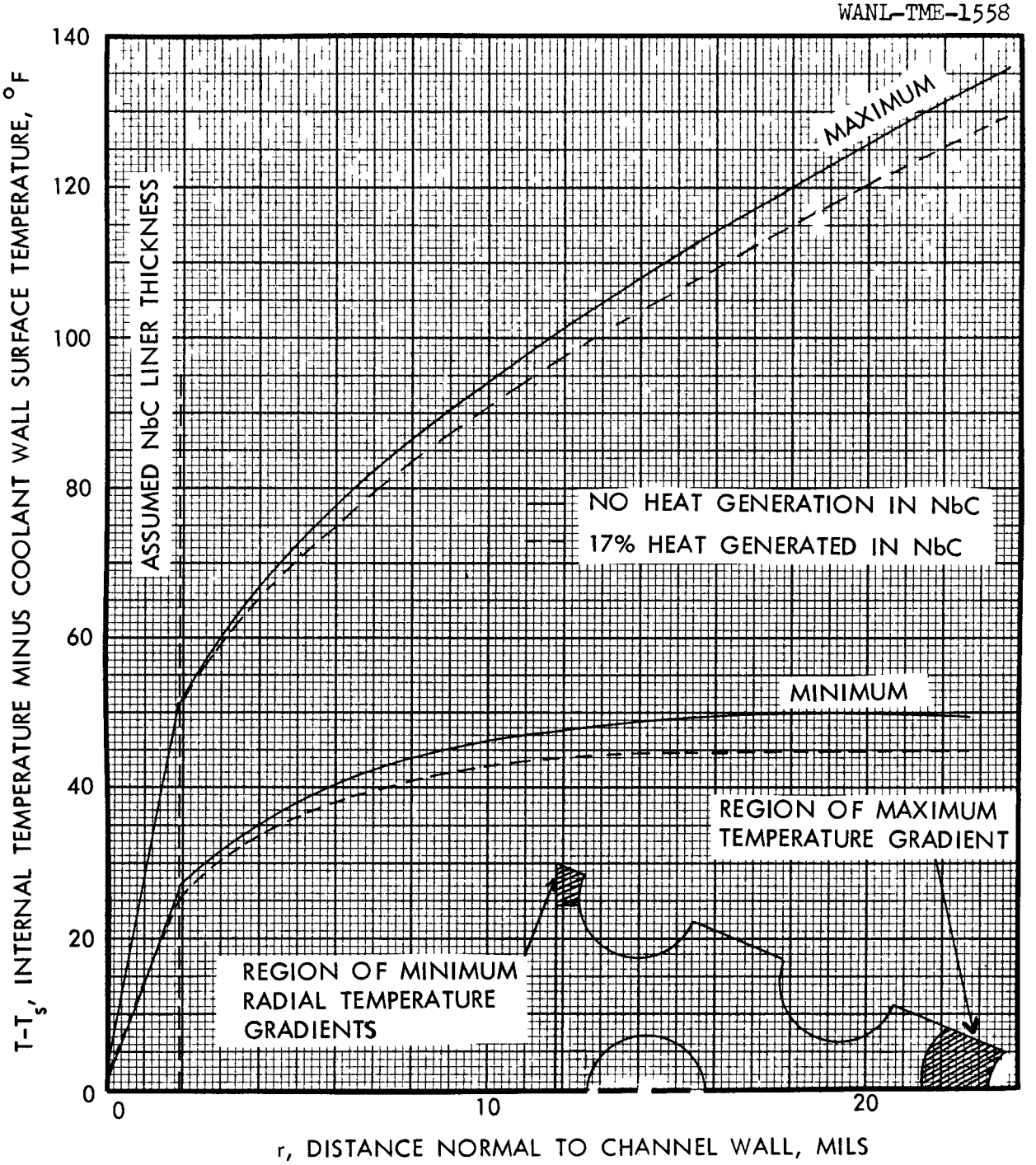

Figure 3

Maximum and Minimum Radial Temperature Gradients
(Normal to Coolant Channel Wall Surface)
With and Without Heat Generation in the NbC Liners
850 KW Total Power Generation

INDUCTION HEATING

Induction heating is accomplished by circulating currents induced in a conducting material when it is located in an alternating magnetic field. The magnitude of the induced currents and electrical resistivity of the material determine the power generated in the form of heat. The most efficient method of induction-heating a workpiece is to insert it in the center of the turns of a coil carrying the alternating current. In this way, the maximum coupling between the magnetic field and the workpiece can be attained.

The induced currents travel circumferentially throughout the cross-section of a cylindrical workpiece, see Figure 4. The distribution of these currents varies from zero at the cylinder axis to a maximum at the surface. The manner in which these currents are distributed is a function of frequency. At higher frequencies the current, following the "skin effect" phenomena, tends to "crowd" toward the surface, causing the greater part of the heat generation in the material near the surface. This phenomena is used, for example, at very high frequencies to heat treat or "case harden" steel components such as gear teeth and pins.

Since current distribution in the workpiece is a function of frequency, the frequency selected can have a considerable effect on the type of heating obtained. Current distribution is usually described in terms of an "effective depth" of penetration, (δ), or "skin depth" which is defined as the distance at which, if the total current were evenly distributed from the surface, the heating effect would be the same as that provided by the actual current distribution.[3] See Figure 5. This effective depth of current penetration in inches is given by the relationship:

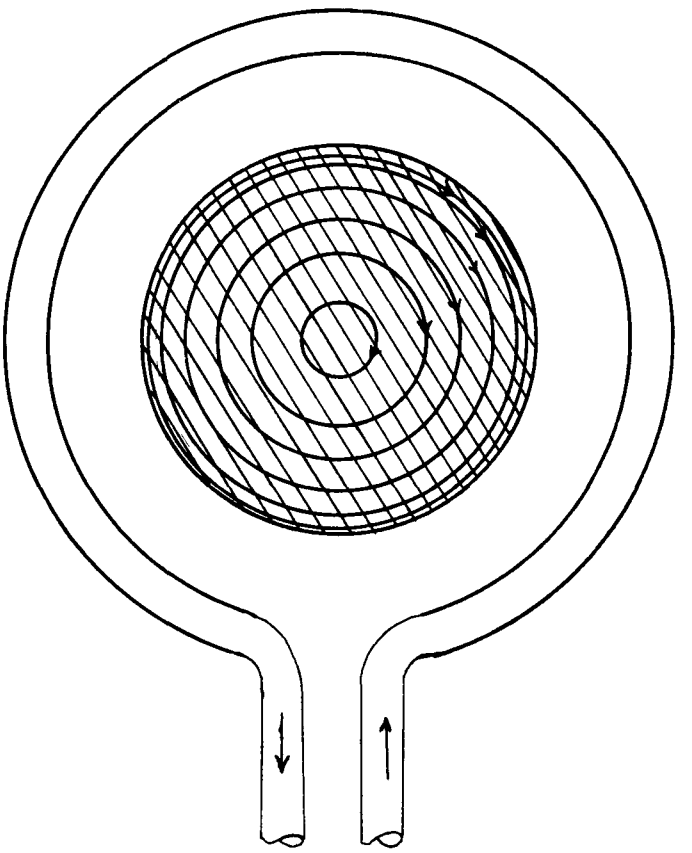

Figure 4

Circumferential Currents in an Inductively Heated Workpiece

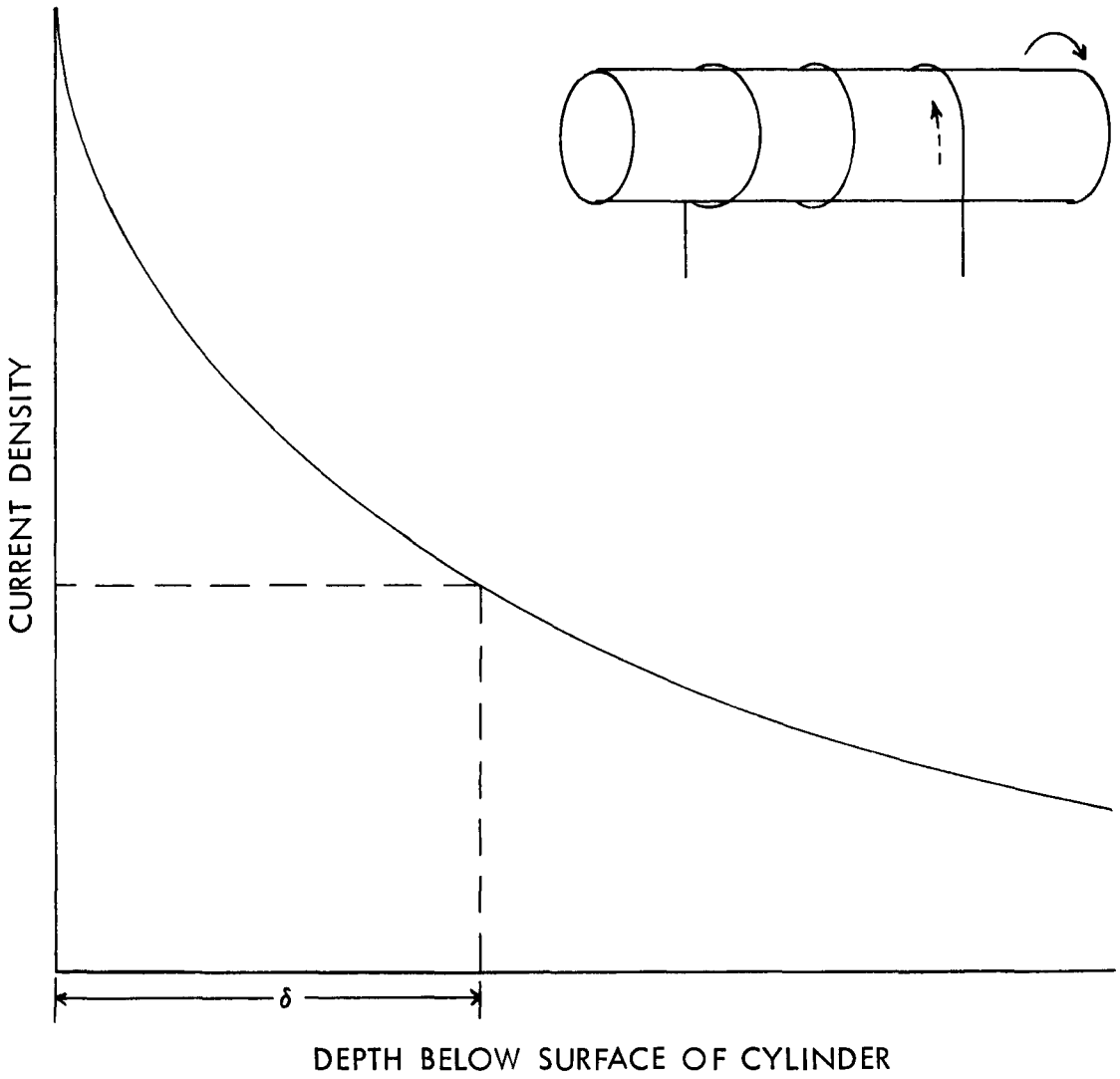

Figure 5

Current Density Distribution in a Cylinder
Current Distribution is Usually Considered
In Terms of the Effective Depth

$$\delta = 1.98\sqrt{\frac{\rho}{\mu \nu}}$$

where ρ is the electrical resistivity in micro ohmcentimeters, μ is the permeability and ν is the frequency.

If through-heating of the workpiece is desired, the most efficient heating is obtained with a skin depth of 1/2 - 1/4 of diameter. For a fuel element cross-section this value of δ can be obtained with a power frequency of 90,000 cycles per second. The distribution of current and power for both high and low frequency heating are shown in Figure 6.[4] Low frequency power is usually generated by rotating machinery in frequencies ranging from 30 to 10,000 cps. High frequency power is generated electronically and ranges from 50 KC to 4 megacycles.

Through-heating of a cylindrical graphite test specimen can be obtained with induction heating if the duration of the heating cycle is long enough and if radiation heat losses from the surface can be minimized.

For fuel element testing, however, induction heating is not a satisfactory method of heating. The cross-section of the element contains a large number of coolant holes through which hydrogen flows at high velocities. With the inherently low power generation rates obtainable with induction heating in the central portion of the rod, that section of the element would be at a relatively low temperature, and the major part of the power generation would be confined

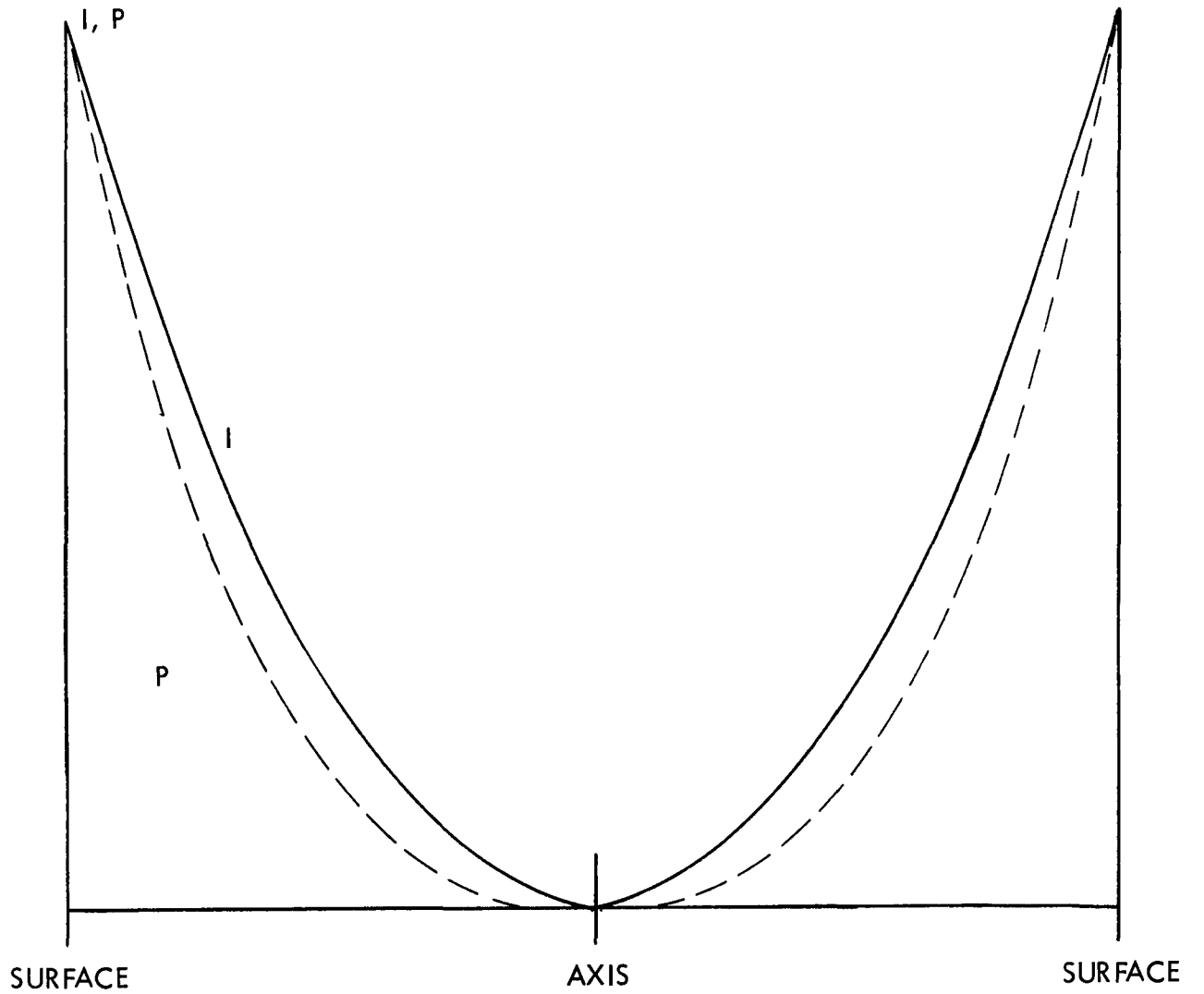

Figure 6

Typical Current and Power Distribution
In a Cylindrical Workpiece

to that annular region of the cross-section with a depth of 1/4 - 1/3 of the diameter. It is only in this region that the desired high temperature would be reached.

The thermal stress problem is obvious and intolerable. Not only would the very large temperature gradient across the section of the element fall short of simulating NERVA conditions, but the fuel element could possibly be ruptured. due to the extreme thermal stresses caused by this gradient.

The power generation distribution from the center of the rod to the surface is a very complex function and can be roughly described as exponential. The use of lower frequencies improve this distribution but a very sharp drop in efficiency occurs as the frequency is reduced. For example, given the graphite rod with a diameter of 0.8", the optimum frequency for through-heating with an efficiency near unity is 90 KC, which is near the minimum frequency obtainable with commerically available r.f. units. If rotating machinery were used; 10 KC is the maximum available frequency in commercially available units and the efficiency would fall below 1/2. This means at least a doubling of capacity and therefore doubling the expense of the power generating system.

Temperature Gradients with Induction Heating

An analysis of the fuel element temperature distributions and temperature gradients was carried out with the TOSS model. Details on the model are discussed in the appendix. The results representing the axial location of highest temperatures for a 850 KW total power input are shown in Figure 7. It is noted that the

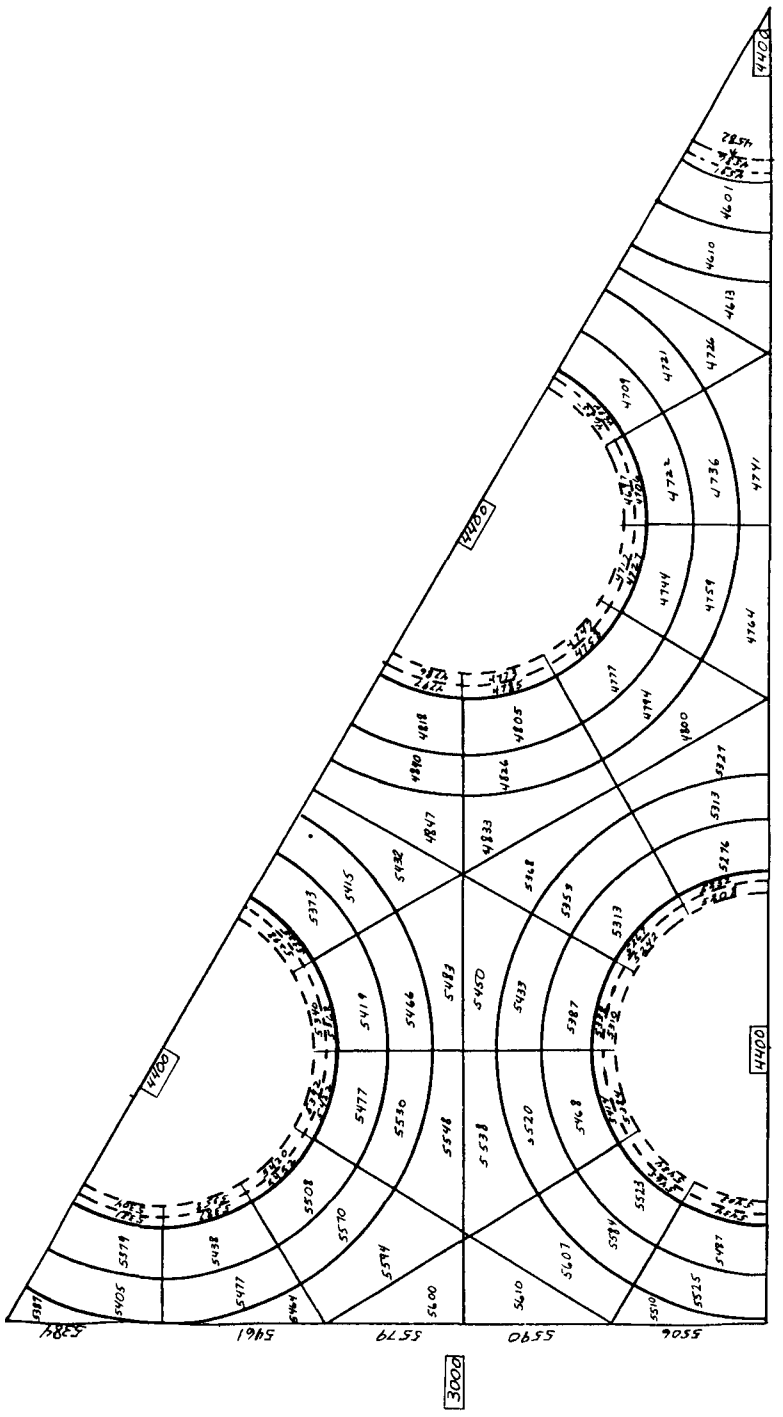

Figure 7

Temperature Distribution in the Fuel Element With
Parabloic Heat Generation; 850 KW
Total Power; Temperature In °R

maximum temperature gradient is 1008°F and that it occurs between the surface of the element and the wall of the central coolant channel. This may be compared with the temperature distributions obtained with equivalent ohmic heating. In the latter case, the maximum temperature is found in the interior of the element and the maximum temperature gradient (between the interior and the surface) found in this case is only 520°F.

It should be pointed out that the temperature distributions obtained depends a great deal on the boundary values chosen. Consequently, even if the absolute temperatures may not correspond exactly to actual conditions, the relative magnitudes serve to point out the differences of the heating methods.

Radiation Heating

Attempts were made to determine the temperature distribution in the fuel element with radiation heating. It was found that in order to maintain the same gas temperature as in the other cases, the boundary temperature for radiation heating had to be excessively high (on the order of 6000°R, not counting radiation losses) such that sublimation of the graphite heating element would be expected. Moreover, the lack of any internal heat generation in the fuel element means that the temperature gradients in this case would be significantly worse than the case for induction heating. It becomes obvious that radiation heating for an entire fuel element containing 19 holes would be both impractical (if not impossible) and undesirable.

COMPARISON OF VARIOUS METHODS AND CONCLUSIONS

Other possible heating methods are passive, external heating, and in-pile heating. In the first mode of heating, the test specimen is heated by a hot gas from a heater mounted in series with the test specimen. This method provides an isothermal condition which may be useful for certain types of tests, but it cannot be used to simulate the reactor temperature profile. The radial cross-sectional temperature gradients are in reverse to those observed for radiation heating, and the temperature gradients would be equally severe. In-pile heating is obviously the ideal method, as it can simulate precisely true reactor conditions. However, the cost of fuel element testing by in-pile heating would be extremely high. Moreover, the turn-around would be slow; thereby precluding its use in quality control tests. A comparison of the various methods is summarized in the following table.

It is concluded that, for fuel element testing, in full or partial lengths, both induction and radiation heating are unsatisfactory and impractical methods of heating.

In the case of resistance (ohmic) heating, the differences in temperature gradients with heat generation in the NbC are negligible when compared to differences in temperature gradients among the various coolant channels. It becomes evident that ohmic heating remains to be the most practical method for large scale testing of fuel elements.

VARIOUS HEATING METHODS FOR FUEL ELEMENT EVALUATION

Heating Methods	Power Generation	Power Generating Equipment Available	Existing Experience	Axial Temperature Distribution	Advantages	Disadvantages
Ohmic	Internal (Uniform in Homogeneous Material)	Yes	Yes	Determined	1. Simplicity 2. Available experience. 3. No channel number limitation.	1. Current conduction chucks. 2. Electric runaway.
Induction	Internal (Skin Effect)	High Cost for Generators (No Procurement)	No	Variable by Coil Spacing.	1. Negative Electric Runaway.	1. Instrumentation Behavior With Inductive Effects. 2. Localized Power Generation. 3. Thermal Shielding and Coil Design.
Radiant	External	Yes	Yes	Arbitrarily Variable	1. Simplicity 2. Removal of Electric Effects. 3. Ability to Control Temperature.	1. Capacity Limited (Radiant Source Temperature)
Passive	External	Procuring	Yes	Constant	1. Simplicity 2. Removal of Electric Effects.	1. Reversed Temperature Gradients in Matrix.
In-Pile	Internal	No	No	Simulatable	1. Represents Potentially the Optimum Simulation.	1. Expensive 2. Slow Turn-Around.

WANL-TME-1558

Astronuclear Laboratory

APPENDIX

TOSS MODEL FOR THE ANALYSIS OF FUEL ELEMENT TEMPERATURE GRADIENTS

Description of Model

The TOSS* model used in the analysis is shown in figure 8. The numbering systems used to identify the various internal, surface, and boundary nodes are given in the figure. Note that the NbC coating, assumed to be 2 mils thick, is divided into two layers. On the scale used in the figure, the nodes in the NbC liner cannot be discerned; consequently, this region is magnified as shown.

The data inputs and dimensions of the nodes are presented in the printouts of a typical case as shown in Table I. Table II gives the printouts of the steady-state solution temperatures.

This model was originally designed to study temperature gradients for ohmic heating with and without heat generation in the NbC coatings. Therefore, the nodal pattern was chosen for its symmetrical properties so as to provide the maximum number of nodes with the same dimensions. This minimizes the calculation of node dimensions.

Ohmic Heating

A total power generation of 850 KW was chosen for this analysis. This yields 1.612×10^5 BTU/In^3-Hr. The volume of the graphite was calculated to be 0.345 $in.^3$ per inch of element. For the case with heat generation in the NbC, the relative heat generation in the graphite was calculated from the following equation:

* Transient or Steady State code. A computer code originally developed at Oak Ridge National Laboratory[5] and modified as described in reference 6.

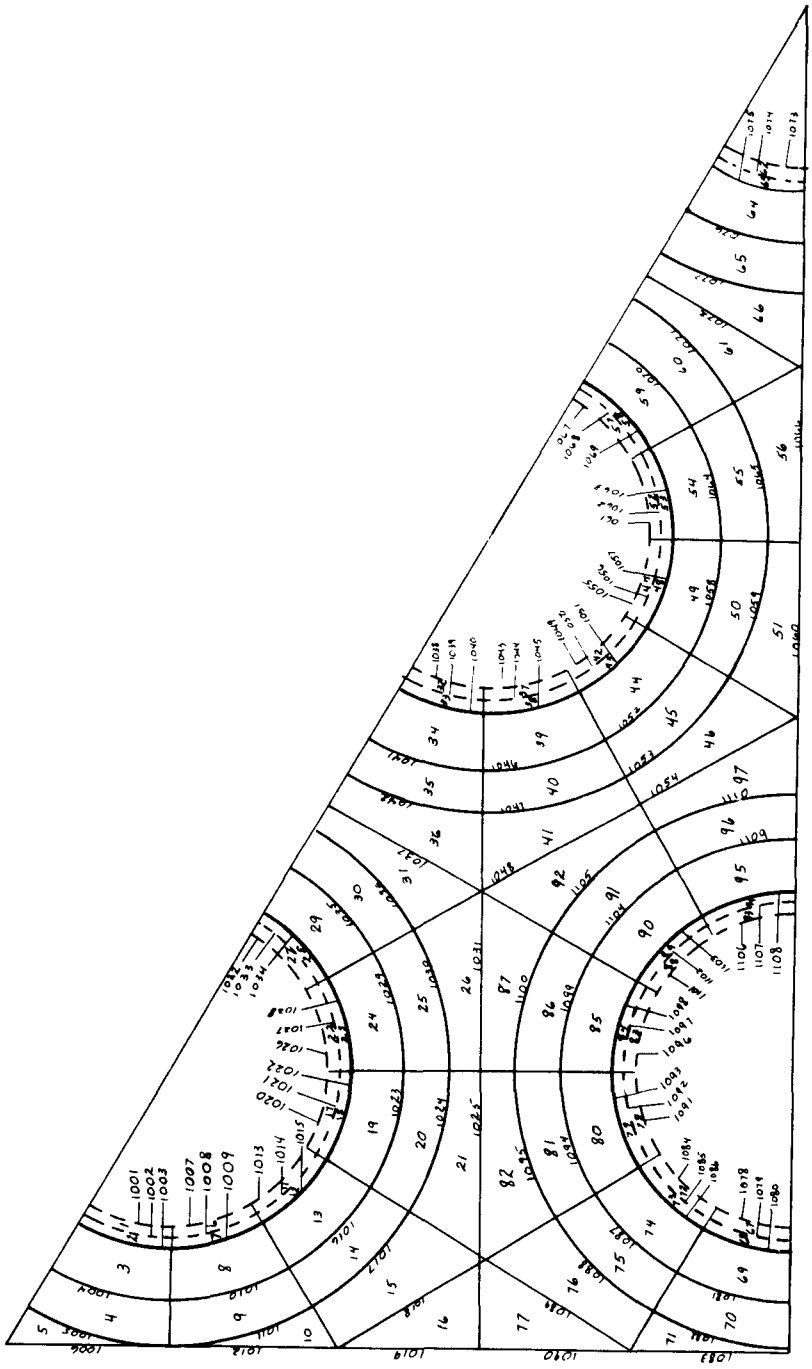

Figure 8

Toss Model for Fuel Element Temperature Distribution
Showing the Nodal and Numbering Systems

Where P = The heat generated

A = The cross-sectional area

ρ = The electrical resistivity.

The subscripts

T = Total

G = Graphite

The ratio $A_{NbC}/A_G = 0.0346$

The ratio ρ_G / ρ_{NbC} is a function of the temperature as shown in Figure 9. At the high temperatures of interest, it approaches a constant of 5.96. From this, it is calculated that 17% of the total heat is generated in the NbC liners.

The boundary temperatures and heat transfer coefficient were based on that occurring at roughly 50 inches in the electrical furnace tests. This resulted in a heat transfer coefficient of 3070 BTU/Hr - Ft^2 - °R. The radiation shield temperature assumed is 3000°R, and the coolant temperature is 4400°R.

Induction Heating

The heat generation in induction heating has a exponential profile with most of the heat generated near the surface of the element. It is evident that the nodal pattern chosen is not ideally suited to the study of induction heating. In order to resolve this problem, the nodes were distributed into 9 groups in a manner shown in Table III. The distribution of heat generation given in the table approximates an exponential function.

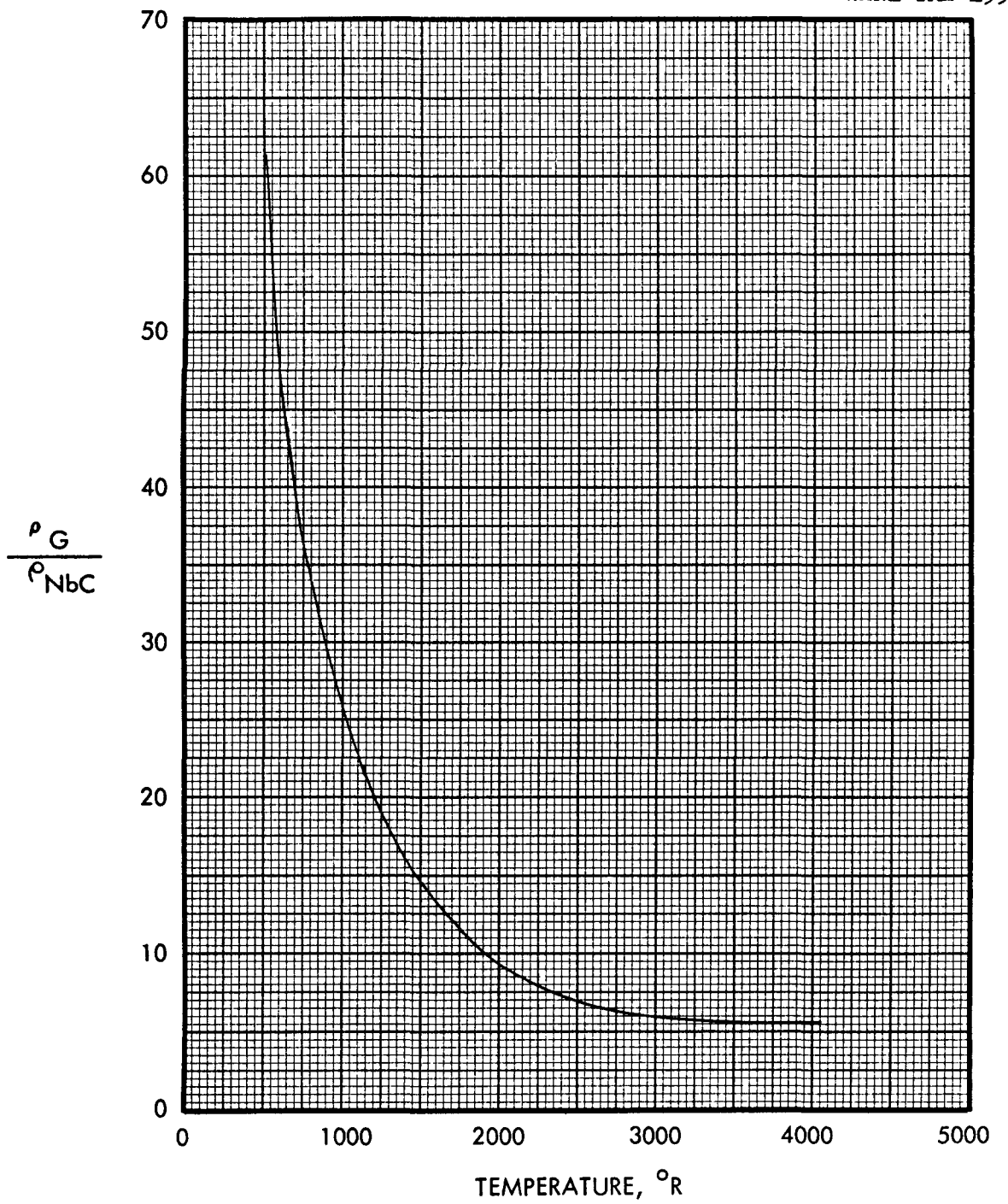

Figure 9

The Effect of Temperature on the Ratio of Electrical Resistivities of Graphite and NbC

REFERENCES

1. "Thermal Analysis of High Temperature Fuel Element Corrosion Tests," R. B. Phillips and G. E. Cort, WANL-TME-744, April, 1964; Also Supplement 1, August, 1965, Supplement 2, May, 1966.

2. "Internal Temperatures of Fuel Elements During Environmental Testing," J. W. H. Chi, J. R. Ferris, and E. A. DeZubay, WANL-TME-565, October 1, 1963.

3. "Application of Induction Heating Power System," W. A. Emerson, Westinghouse Engineers, July, 1965.

4. "Induction Heating," P. G. Simpson, McGraw Hill Book Company, New York, 1960.

5. "TOSS an IBM-7090 Code for Computing Transient or Steady State Temperature Distributions," Union Carbide Nuclear Co. K-1494, December, 1961.

6. "Modified Transient and for Steady State (TOSS) Digital Heat Transfer Code," B. L. Pierce, WANL-TME-1108, April, 1964.

Table I

Data Inputs to Toss Model for Ohmic Heating, 850 KW
With Heat Generation in NbC Liners

INITIAL TIME	FINAL TIME	TIME INCREMENT	CONVERGE CRITERIA	CONVERGE AFTER	TYPE	
0.	C.	0.0100	0.1000	-0.	2	1

BOUNDARY AND SURFACE TEMPERATURES

NODE	TEMP	NODE	TEMP	NODE	TEMP	NODE	TEMP	NODE	TEMP
1001	4500.00	1002	4500.00	1003	4500.00	1004	4500.00	1005	4500.00
1006	4500.00	1007	4500.00	1008	4500.00	1009	4500.00	1010	4500.00
1011	4500.00	1012	4500.00	1013	4500.00	1014	4500.00	1015	4500.00
1016	4500.00	1017	4500.00	1018	4500.00	1019	4500.00	1020	4500.00
1021	4500.00	1022	4500.00	1023	4500.00	1024	4500.00	1025	4500.00
1026	4500.00	1027	4500.00	1028	4500.00	1029	4500.00	1030	4500.00
1031	4500.00	1032	4500.00	1033	4500.00	1034	4500.00	1035	4500.00
1036	4500.00	1037	4500.00	1038	4500.00	1039	4500.00	1040	4500.00
1041	4500.00	1042	4500.00	1043	4500.00	1044	4500.00	1045	4500.00
1046	4500.00	1047	4500.00	1048	4500.00	1049	4500.00	1050	4500.00
1051	4500.00	1052	4500.00	1053	4500.00	1054	4500.00	1055	4500.00
1056	4500.00	1057	4500.00	1058	4500.00	1059	4500.00	1060	4500.00
1061	4500.00	1062	4500.00	1063	4500.00	1064	4500.00	1065	4500.00
1066	4500.00	1067	4500.00	1068	4500.00	1069	4500.00	1070	4500.00
1071	4500.00	1072	4500.00	1073	4500.00	1074	4500.00	1075	4500.00
1076	4500.00	1077	4500.00	1078	4500.00	1079	4500.00	1080	4500.00
1081	4500.00	1082	4500.00	1083	4500.00	1084	4500.00	1085	4500.00
1086	4500.00	1087	4500.00	1088	4500.00	1089	4500.00	1090	4500.00
1091	4500.00	1092	4500.00	1093	4500.00	1094	4500.00	1095	4500.00
1096	4500.00	1097	4500.00	1098	4500.00	1099	4500.00	1100	4500.00
1101	4500.00	1102	4500.00	1103	4500.00	1104	4500.00	1105	4500.00
1106	4500.00	1107	4500.00	1108	4500.00	1109	4500.00	1110	4500.00
2001	4400.00	2002	3000.00	2003	4400.00	2004	4400.00	2005	4400.00

BOUNDARY TEMPERATURE TABLES

NODE	TEMP	TIME	TEMP	TIME	TEMP	TIME	TEMP	TIME	TEMP	TIME

MATERIALS

	NO.	HEAT CAP.	DENSITY	CONDUCTIVITY
NBC	21	0.0700	0.2820	8.2000

INTERNAL NODES

WANL-TME-1558

Table I (Continued)

NODE	MATERIAL		LENGTH	WIDTH	PTH	VOLUME	BASE GLN.	APACITY
1	NBC	21	0.0140	0.0010	1.0000	0.0000	0.7950E 06	0.1658E-04
2	NBC	21	0.0140	0.0010	1.0000	0.0000	0.7950E 06	0.1658E-04
3	GRAPH	1	0.0293	0.0138	1.0000	0.0004	0.1337E 06	0.8584E-03
4	GRAPH	1	0.0565	0.0142	1.0000	0.0008	0.1337E 06	0.1703E-02
5	GRAPH	1	0.0375	0.0020	1.0000	0.0001	0.1337E 06	0.1592E-03
6	NBC	21	0.0140	0.0010	1.0000	0.0000	0.7950E 06	0.1658E-04
7	NBC	21	0.0140	0.0010	1.0000	0.0000	0.7950E 06	0.1658E-04
8	GRAPH	1	0.0293	0.0138	1.0000	0.0004	0.1337E 06	0.8584E-03
9	GRAPH	1	0.0565	0.0152	1.0000	0.0009	0.1337E 06	0.1823E-02
10	GRAPH	1	0.0375	0.0020	1.0000	0.0001	0.1337E 06	0.1592E-03
11	NBC	21	0.0140	0.0010	1.0000	0.0000	0.7950E 06	0.1658E-04
12	NBC	21	0.0140	0.0010	1.0000	0.0000	0.7950E 06	0.1658E-04
13	GRAPH	1	0.0293	0.0138	1.0000	0.0004	0.1337E 06	0.8584E-03
14	GRAPH	1	0.0565	0.0152	1.0000	0.0009	0.1337E 06	0.1823E-02
15	GRAPH	1	0.0378	0.0142	1.0000	0.0005	0.1337E 06	0.1139E-02
16	GRAPH	1	0.0405	0.0142	1.0000	0.0006	0.1337E 06	0.1221E-02
17	NBC	21	0.0140	0.0010	1.0000	0.0000	0.7950E 06	0.1658E-04
18	NBC	21	0.0140	0.0010	1.0000	0.0000	0.7950E 06	0.1658E-04
19	GRAPH	1	0.0293	0.0138	1.0000	0.0004	0.1337E 06	0.8584E-03
20	GRAPH	1	0.0565	0.0152	1.0000	0.0009	0.1337E 06	0.1823E-02
21	GRAPH	1	0.0378	0.0142	1.0000	0.0005	0.1337E 06	0.1139E-02
22	NBC	21	0.0140	0.0010	1.0000	0.0000	0.7950E 06	0.1658E-04
23	NBC	21	0.0140	0.0010	1.0000	0.0000	0.7950E 06	0.1658E-04
24	GRAPH	1	0.0293	0.0138	1.0000	0.0004	0.1337E 06	0.8584E-03
25	GRAPH	1	0.0565	0.0152	1.0000	0.0009	0.1337E 06	0.1823E-02
26	GRAPH	1	0.0378	0.0142	1.0000	0.0005	0.1337E 06	0.1139E-02
27	NBC	21	0.0140	0.0010	1.0000	0.0000	0.7950E 06	0.1658E-04
28	NBC	21	0.0140	0.0010	1.0000	0.0000	0.7950E 06	0.1658E-04
29	GRAPH	1	0.0293	0.0138	1.0000	0.0004	0.1337E 06	0.8584E-03
30	GRAPH	1	0.0565	0.0152	1.0000	0.0009	0.1337E 06	0.1823E-02
31	GRAPH	1	0.0378	0.0142	1.0000	0.0005	0.1337E 06	0.1139E-02
32	NBC	21	0.0140	0.0010	1.0000	0.0000	0.7950E 06	0.1658E-04
33	NBC	21	0.0140	0.0010	1.0000	0.0000	0.7950E 06	0.1658E-04
34	GRAPH	1	0.0293	0.0138	1.0000	0.0004	0.1337E 06	0.8584E-03
35	GRAPH	1	0.0565	0.0152	1.0000	0.0009	0.1337E 06	0.1823E-02
36	GRAPH	1	0.0378	0.0142	1.0000	0.0005	0.1337E 06	0.1139E-02
37	NBC	21	0.0140	0.0010	1.0000	0.0000	0.7950E 06	0.1658E-04
38	NBC	21	0.0140	0.0010	1.0000	0.0000	0.7950E 06	0.1658E-04
39	GRAPH	1	0.0293	0.0138	1.0000	0.0004	0.1337E 06	0.8584E-03
40	GRAPH	1	0.0565	0.0152	1.0000	0.0009	0.1337E 06	0.1823E-02
41	GRAPH	1	0.0378	0.0142	1.0000	0.0005	0.1337E 06	0.1139E-02
42	NBC	21	0.0140	0.0010	1.0000	0.0000	0.7950E 06	0.1658E-04
43	NBC	21	0.0140	0.0010	1.0000	0.0000	0.7950E 06	0.1658E-04
44	GRAPH	1	0.0293	0.0138	1.0000	0.0004	0.1337E 06	0.8584E-03
45	GRAPH	1	0.0565	0.0152	1.0000	0.0009	0.1337E 06	0.1823E-02
46	GRAPH	1	0.0378	0.0142	1.0000	0.0005	0.1337E 06	0.1139E-02

Table I (Continued)

47	NBC	21	0.0140	0.0010	.0000	0.0000	0.7950E 06	658E-04
48	NBC	21	0.0140	0.0010	1.0000	0.0000	0.7950E 06	0.1658E-04
49	GRAPH	1	0.0293	0.0138	1.0000	0.0004	0.1337E 06	0.8584E-03
50	GRAPH	1	0.0565	0.0152	1.0000	0.0009	0.1337E 06	0.1823E-02
51	GRAPH	1	0.0378	0.0142	1.0000	0.0005	0.1337E 06	0.1139E-02
52	NBC	21	0.0140	0.0010	1.0000	0.0000	0.7950E 06	0.1658E-04
53	NBC	21	0.0140	0.0010	1.0000	0.0000	0.7950E 06	0.1658E-04
54	GRAPH	1	0.0293	0.0138	1.0000	0.0004	0.1337E 06	0.8584E-03
55	GRAPH	1	0.0565	0.0152	1.0000	0.0009	0.1337E 06	0.1823E-02
56	GRAPH	1	0.0378	0.0142	1.0000	0.0005	0.1337E 06	0.1139E-02
57	NBC	21	0.0140	0.0010	1.0000	0.0000	0.7950E 06	0.1658E-04
58	NBC	21	0.0140	0.0010	1.0000	0.0000	0.7950E 06	0.1658E-04
59	GRAPH	1	0.0293	0.0138	1.0000	0.0004	0.1337E 06	0.8584E-03
60	GRAPH	1	0.0565	0.0152	1.0000	0.0009	0.1337E 06	0.1823E-02
61	GRAPH	1	0.0378	0.0142	1.0000	0.0005	0.1337E 06	0.1139E-02
62	NBC	21	0.0140	0.0010	1.0000	0.0000	0.7950E 06	0.1658E-04
63	NBC	21	0.0140	0.0010	1.0000	0.0000	0.7950E 06	0.1658E-04
64	GRAPH	1	0.0293	0.0138	1.0000	0.0004	0.1337E 06	0.8584E-03
65	GRAPH	1	0.0565	0.0152	1.0000	0.0009	0.1337E 06	0.1823E-02
66	GRAPH	1	0.0378	0.0142	1.0000	0.0005	0.1337E 06	0.1139E-02
67	NBC	21	0.0140	0.0010	1.0000	0.0000	0.7950E 06	0.1658E-04
68	NBC	21	0.0140	0.0010	1.0000	0.0000	0.7950E 06	0.1658E-04
69	GRAPH	1	0.0293	0.0138	1.0000	0.0004	0.1337E 06	0.8584E-03
70	GRAPH	1	0.0565	0.0152	1.0000	0.0009	0.1337E 06	0.1823E-02
71	GRAPH	1	0.0375	0.0020	1.0000	0.0001	0.1337E 06	0.1592E-03
72	NBC	21	0.0140	0.0010	1.0000	0.0000	0.7950E 06	0.1658E-04
73	NBC	21	0.0140	0.0010	1.0000	0.0000	0.7950E 06	0.1658E-04
74	GRAPH	1	0.0293	0.0138	1.0000	0.0004	0.1337E 06	0.8584E-03
75	GRAPH	1	0.0565	0.0152	1.0000	0.0009	0.1337E 06	0.1823E-02
76	GRAPH	1	0.0378	0.0142	1.0000	0.0005	0.1337E 06	0.1139E-02
77	GRAPH	1	0.0405	0.0142	1.0000	0.0006	0.1337E 06	0.1221E-02
78	NBC	21	0.0140	0.0010	1.0000	0.0000	0.7950E 06	0.1658E-04
79	NBC	21	0.0140	0.0010	1.0000	0.0000	0.7950E 06	0.1658E-04
80	GRAPH	1	0.0293	0.0138	1.0000	0.0004	0.1337E 06	0.8584E-03
81	GRAPH	1	0.0565	0.0152	1.0000	0.0009	0.1337E 06	0.1823E-02
82	GRAPH	1	0.0378	0.0142	1.0000	0.0005	0.1337E 06	0.1139E-02
83	NBC	21	0.0140	0.0010	1.0000	0.0000	0.7950E 06	0.1658E-04
84	NBC	21	0.0140	0.0010	1.0000	0.0000	0.7950E 06	0.1658E-04
85	GRAPH	1	0.0293	0.0138	1.0000	0.0004	0.1337E 06	0.8584E-03
86	GRAPH	1	0.0565	0.0152	1.0000	0.0009	0.1337E 06	0.1823E-02
87	GRAPH	1	0.0378	0.0142	1.0000	0.0005	0.1337E 06	0.1139E-02
88	NBC	21	0.0140	0.0010	1.0000	0.0000	0.7950E 06	0.1658E-04
89	NBC	21	0.0140	0.0010	1.0000	0.0000	0.7950E 06	0.1658E-04
90	GRAPH	1	0.0293	0.0138	1.0000	0.0004	0.1337E 06	0.8584E-03
91	GRAPH	1	0.0565	0.0152	1.0000	0.0009	0.1337E 06	0.1823E-02
	GRAPH	1	0.0378	0.0142	1.0000	0.0005	0.1337E 06	0.1139E-02
		21	0.0140	0.0010	1.0000	0.0000	0.7950E 06	0.1658E-04

94	NBC	21	0.0140	0.0010	0000	0.0000	0.7950E 06	658E-04
95	GRAPH	1	0.0293	0.0138	1.0000	0.0004	0.1337E 06	0.8584E-03
96	GRAPH	1	0.0565	0.0152	1.0000	0.0009	0.1337E 06	0.1823E-02
97	GRAPH	1	0.0378	0.0142	1.0000	0.0005	0.1337E 06	0.1139E-02

INTERNAL CONNECTORS

NODES		MATERIAL		LENGTH	MATERIAL		LENGTH	WIDTH	DEPTH
1	2	NBC	21	0.0005	NBC	21	0.0005	0.0140	1.0000
2	3	NBC	21	0.0005	GRAPH	1	0.0069	0.0293	1.0000
3	4	GRAPH	1	0.0069	GRAPH	1	0.0071	0.0429	1.0000
4	5	GRAPH	1	0.0071	GRAPH	1	0.0010	0.0565	1.0000
6	7	NBC	21	0.0005	NBC	21	0.0005	0.0140	1.0000
7	8	NBC	21	0.0005	GRAPH	1	0.0069	0.0293	1.0000
8	9	GRAPH	1	0.0069	GRAPH	1	0.0071	0.0429	1.0000
9	10	GRAPH	1	0.0071	GRAPH	1	0.0010	0.0565	1.0000
11	12	NBC	21	0.0005	NBC	21	0.0005	0.0140	1.0000
12	13	NBC	21	0.0005	GRAPH	1	0.0069	0.0293	1.0000
13	14	GRAPH	1	0.0069	GRAPH	1	0.0071	0.0429	1.0000
14	15	GRAPH	1	0.0071	GRAPH	1	0.0071	0.0471	1.0000
15	16	GRAPH	1	0.0071	GRAPH	1	0.0071	0.0405	1.0000
17	18	NBC	21	0.0005	NBC	21	0.0005	0.0140	1.0000
18	19	NBC	21	0.0005	GRAPH	1	0.0069	0.0293	1.0000
19	20	GRAPH	1	0.0069	GRAPH	1	0.0071	0.0429	1.0000
20	21	GRAPH	1	0.0071	GRAPH	1	0.0071	0.0471	1.0000
22	23	NBC	21	0.0005	NBC	21	0.0005	0.0140	1.0000
23	24	NBC	21	0.0005	GRAPH	1	0.0069	0.0293	1.0000
24	25	GRAPH	1	0.0069	GRAPH	1	0.0071	0.0429	1.0000
25	26	GRAPH	1	0.0071	GRAPH	1	0.0071	0.0471	1.0000
27	28	NBC	21	0.0005	NBC	21	0.0005	0.0140	1.0000
28	29	NBC	21	0.0005	GRAPH	1	0.0069	0.0293	1.0000
29	30	GRAPH	1	0.0069	GRAPH	1	0.0071	0.0429	1.0000
30	31	GRAPH	1	0.0071	GRAPH	1	0.0071	0.0471	1.0000
32	33	NBC	21	0.0005	NBC	21	0.0005	0.0140	1.0000
33	34	NBC	21	0.0005	GRAPH	1	0.0069	0.0293	1.0000
34	35	GRAPH	1	0.0069	GRAPH	1	0.0071	0.0429	1.0000
35	36	GRAPH	1	0.0071	GRAPH	1	0.0071	0.0471	1.0000
37	38	NBC	21	0.0005	NBC	21	0.0005	0.0140	1.0000
38	39	NBC	21	0.0005	GRAPH	1	0.0069	0.0293	1.0000
39	40	GRAPH	1	0.0069	GRAPH	1	0.0071	0.0429	1.0000
40	41	GRAPH	1	0.0071	GRAPH	1	0.0071	0.0471	1.0000
42	43	NBC	21	0.0005	NBC	21	0.0005	0.0140	1.0000
43	44	NBC	21	0.0005	GRAPH	1	0.0069	0.0293	1.0000
44	45	GRAPH	1	0.0069	GRAPH	1	0.0071	0.0429	1.0000
45	46	GRAPH	1	0.0071	GRAPH	1	0.0071	0.0471	1.0000
47	48	NBC	21	0.0005	NBC	21	0.0005	0.0140	1.0000
48	49	NBC	21	0.0005	GRAPH	1	0.0069	0.0293	1.0000
49	50	GRAPH	1	0.0069	GRAPH	1	0.0071	0.0429	1.0000

Table I (Continued)

5.	51	GRAPH	1	0.0071	GRAPH		0.0071	0.0471	1.0000
52	53	NBC	21	0.0005	NBC	21	0.0005	0.0140	1.0000
53	54	NBC	21	0.0005	GRAPH	1	0.0069	0.0293	1.0000
54	55	GRAPH	1	0.0069	GRAPH	1	0.0071	0.0429	1.0000
55	56	GRAPH	1	0.0071	GRAPH	1	0.0071	0.0471	1.0000
57	58	NBC	21	0.0005	NBC	21	0.0005	0.0140	1.0000
58	59	NBC	21	0.0005	GRAPH	1	0.0069	0.0293	1.0000
59	60	GRAPH	1	0.0069	GRAPH	1	0.0071	0.0429	1.0000
60	61	GRAPH	1	0.0071	GRAPH	1	0.0071	0.0471	1.0000
62	63	NBC	21	0.0005	NBC	21	0.0005	0.0140	1.0000
63	64	NBC	21	0.0005	GRAPH	1	0.0069	0.0293	1.0000
64	65	GRAPH	1	0.0069	GRAPH	1	0.0071	0.0429	1.0000
65	66	GRAPH	1	0.0071	GRAPH	1	0.0071	0.0471	1.0000
67	68	NBC	21	0.0005	NBC	21	0.0005	0.0140	1.0000
68	69	NBC	21	0.0005	GRAPH	1	0.0069	0.0293	1.0000
69	70	GRAPH	1	0.0069	GRAPH	1	0.0071	0.0429	1.0000
70	71	GRAPH	1	0.0071	GRAPH	1	0.0010	0.0565	1.0000
72	73	NBC	21	0.0005	NBC	21	0.0005	0.0140	1.0000
73	74	NBC	21	0.0005	GRAPH	1	0.0069	0.0293	1.0000
74	75	GRAPH	1	0.0069	GRAPH	1	0.0071	0.0429	1.0000
75	76	GRAPH	1	0.0071	GRAPH	1	0.0071	0.0471	1.0000
76	77	GRAPH	1	0.0071	GRAPH	1	0.0071	0.0405	1.0000
78	79	NBC	21	0.0005	NBC	21	0.0005	0.0140	1.0000
79	80	NBC	21	0.0005	GRAPH	1	0.0069	0.0293	1.0000
80	81	GRAPH	1	0.0069	GRAPH	1	0.0071	0.0429	1.0000
81	82	GRAPH	1	0.0071	GRAPH	1	0.0071	0.0471	1.0000
83	84	NBC	21	0.0005	NBC	21	0.0005	0.0140	1.0000
84	85	NBC	21	0.0005	GRAPH	1	0.0069	0.0293	1.0000
85	86	GRAPH	1	0.0069	GRAPH	1	0.0071	0.0429	1.0000
86	87	GRAPH	1	0.0071	GRAPH	1	0.0071	0.0471	1.0000
88	89	NBC	21	0.0005	NBC	21	0.0005	0.0140	1.0000
89	90	NBC	21	0.0005	GRAPH	1	0.0069	0.0293	1.0000
90	91	GRAPH	1	0.0069	GRAPH	1	0.0071	0.0429	1.0000
91	92	GRAPH	1	0.0071	GRAPH	1	0.0071	0.0471	1.0000
93	94	NBC	21	0.0005	NBC	21	0.0005	0.0140	1.0000
94	95	NBC	21	0.0005	GRAPH	1	0.0069	0.0293	1.0000
95	96	GRAPH	1	0.0069	GRAPH	1	0.0071	0.0429	1.0000
96	97	GRAPH	1	0.0071	GRAPH	1	0.0071	0.0471	1.0000
1	6	NBC	21	0.0070	NBC	21	0.0070	0.0010	1.0000
2	7	NBC	21	0.0070	NBC	21	0.0070	0.0010	1.0000
3	8	GRAPH	1	0.0146	GRAPH	1	0.0146	0.0138	1.0000
4	9	GRAPH	1	0.0282	GRAPH	1	0.0282	0.0142	1.0000
6	11	NBC	21	0.0070	NBC	21	0.0070	0.0010	1.0000
7	12	NBC	21	0.0070	NBC	21	0.0070	0.0010	1.0000
8	13	GRAPH	1	0.0146	GRAPH	1	0.0146	0.0138	1.0000
9	14	GRAPH	1	0.0282	GRAPH	1	0.0282	0.0142	1.0000
10	15	GRAPH	1	0.0187	GRAPH	1	0.0189	0.0142	1.0000

Table I (Continued)

11	17	NBC	21	0.0070	NBC	21	0.0070	0.0010	1.0000
12	18	NBC	21	0.0070	NBC	21	0.0070	0.0010	1.0000
13	19	GRAPH	1	0.0146	GRAPH	1	0.0146	0.0138	1.0000
14	20	GRAPH	1	0.0282	GRAPH	1	0.0282	0.0142	1.0000
15	21	GRAPH	1	0.0189	GRAPH	1	0.0189	0.0142	1.0000
17	22	NBC	21	0.0070	NBC	21	0.0070	0.0010	1.0000
18	23	NBC	21	0.0070	NBC	21	0.0070	0.0010	1.0000
19	24	GRAPH	1	0.0146	GRAPH	1	0.0146	0.0138	1.0000
20	25	GRAPH	1	0.0282	GRAPH	1	0.0282	0.0142	1.0000
21	26	GRAPH	1	0.0189	GRAPH	1	0.0189	0.0142	1.0000
22	27	NBC	21	0.0070	NBC	21	0.0070	0.0010	1.0000
23	28	NBC	21	0.0070	NBC	21	0.0070	0.0010	1.0000
24	29	GRAPH	1	0.0146	GRAPH	1	0.0146	0.0138	1.0000
25	30	GRAPH	1	0.0282	GRAPH	1	0.0282	0.0142	1.0000
26	31	GRAPH	1	0.0189	GRAPH	1	0.0189	0.0142	1.0000
32	37	NBC	21	0.0070	NBC	21	0.0070	0.0010	1.0000
33	38	NBC	21	0.0070	NBC	21	0.0070	0.0010	1.0000
34	39	GRAPH	1	0.0146	GRAPH	1	0.0146	0.0138	1.0000
35	40	GRAPH	1	0.0282	GRAPH	1	0.0282	0.0142	1.0000
36	41	GRAPH	1	0.0189	GRAPH	1	0.0189	0.0142	1.0000
37	42	NBC	21	0.0070	NBC	21	0.0070	0.0010	1.0000
38	43	NBC	21	0.0070	NBC	21	0.0070	0.0010	1.0000
39	44	GRAPH	1	0.0146	GRAPH	1	0.0146	0.0138	1.0000
40	45	GRAPH	1	0.0282	GRAPH	1	0.0282	0.0142	1.0000
41	46	GRAPH	1	0.0189	GRAPH	1	0.0189	0.0142	1.0000
42	47	NBC	21	0.0070	NBC	21	0.0070	0.0010	1.0000
43	48	NBC	21	0.0070	NBC	21	0.0070	0.0010	1.0000
44	49	GRAPH	1	0.0146	GRAPH	1	0.0146	0.0138	1.0000
45	50	GRAPH	1	0.0282	GRAPH	1	0.0282	0.0142	1.0000
46	51	GRAPH	1	0.0189	GRAPH	1	0.0189	0.0142	1.0000
47	52	NBC	21	0.0070	NBC	21	0.0070	0.0010	1.0000
48	53	NBC	21	0.0070	NBC	21	0.0070	0.0010	1.0000
49	54	GRAPH	1	0.0146	GRAPH	1	0.0146	0.0138	1.0000
50	55	GRAPH	1	0.0282	GRAPH	1	0.0282	0.0142	1.0000
51	56	GRAPH	1	0.0189	GRAPH	1	0.0189	0.0142	1.0000
52	57	NBC	21	0.0070	NBC	21	0.0070	0.0010	1.0000
53	58	NBC	21	0.0070	NBC	21	0.0070	0.0010	1.0000
54	59	GRAPH	1	0.0146	GRAPH	1	0.0146	0.0138	1.0000
55	60	GRAPH	1	0.0282	GRAPH	1	0.0282	0.0142	1.0000
56	61	GRAPH	1	0.0189	GRAPH	1	0.0189	0.0142	1.0000
67	72	NBC	21	0.0070	NBC	21	0.0070	0.0010	1.0000
68	73	NBC	21	0.0070	NBC	21	0.0070	0.0010	1.0000
69	74	GRAPH	1	0.0146	GRAPH	1	0.0146	0.0138	1.0000
70	75	GRAPH	1	0.0282	GRAPH	1	0.0282	0.0142	1.0000
71	76	GRAPH	1	0.0189	GRAPH	1	0.0189	0.0142	1.0000
72	78	NBC	21	0.0070	NBC	21	0.0070	0.0010	1.0000
73	79	NBC	21	0.0070	NBC	21	0.0070	0.0010	1.0000

Astronuclear Laboratory
WANL-TME-1558

Table I (Continued)

74	80	GRAPH	1	0.0146	GRAPH		0.0146	0.0138	1.0000	
75	81	GRAPH	1	0.0282	GRAPH	1	0.0282	0.0142	1.0000	
76	82	GRAPH	1	0.0189	GRAPH	1	0.0189	0.0142	1.0000	
77	16	GRAPH	1	0.0202	GRAPH	1	0.0202	0.0142	1.0000	
78	83	NBC	21	0.0070	NBC	21	0.0070	0.0010	1.0000	
79	84	NBC	21	0.0070	NBC	21	0.0070	0.0010	1.0000	
80	85	GRAPH	1	0.0146	GRAPH	1	0.0146	0.0138	1.0000	
81	86	GRAPH	1	0.0282	GRAPH	1	0.0282	0.0142	1.0000	
82	87	GRAPH	1	0.0189	GRAPH	1	0.0189	0.0142	1.0000	
83	88	NBC	21	0.0070	NBC	21	0.0070	0.0010	1.0000	
84	89	NBC	21	0.0070	NBC	21	0.0070	0.0010	1.0000	
85	90	GRAPH	1	0.0146	GRAPH	1	0.0146	0.0138	1.0000	
86	91	GRAPH	1	0.0282	GRAPH	1	0.0282	0.0142	1.0000	
87	92	GRAPH	1	0.0189	GRAPH	1	0.0189	0.0142	1.0000	
88	93	NBC	21	0.0070	NBC	21	0.0070	0.0010	1.0000	
89	94	NBC	21	0.0070	NBC	21	0.0070	0.0010	1.0000	
90	95	GRAPH	1	0.0146	GRAPH	1	0.0146	0.0138	1.0000	
91	96	GRAPH	1	0.0282	GRAPH	1	0.0282	0.0142	1.0000	
92	97	GRAPH	1	0.0189	GRAPH	1	0.0189	0.0142	1.0000	
1	1001	NBC	21	0.0005				0.0140	1.0000	
6	1007	NBC	21	0.0005				0.0140	1.0000	
11	1013	NBC	21	0.0005				0.0140	1.0000	
17	1020	NBC	21	0.0005				0.0140	1.0000	
22	1026	NBC	21	0.0005				0.0140	1.0000	
27	1032	NBC	21	0.0005				0.0140	1.0000	
32	1038	NBC	21	0.0005				0.0140	1.0000	
37	1043	NBC	21	0.0005				0.0140	1.0000	
42	1049	NBC	21	0.0005				0.0140	1.0000	
47	1055	NBC	21	0.0005				0.0140	1.0000	
52	1061	NBC	21	0.0005				0.0140	1.0000	
57	1067	NBC	21	0.0005				0.0140	1.0000	
62	1073	NBC	21	0.0005				0.0140	1.0000	
67	1078	NBC	21	0.0005				0.0140	1.0000	
72	1084	NBC	21	0.0005				0.0140	1.0000	
78	1091	NBC	21	0.0005				0.0140	1.0000	
83	1096	NBC	21	0.0005				0.0140	1.0000	
88	1101	NBC	21	0.0005				0.0140	1.0000	
93	1106	NBC	21	0.0005				0.0140	1.0000	
71	1083	GRAPH	1	0.0010				0.0565	1.0000	
77	1090	GRAPH	1	0.0071				0.0405	1.0000	
16	1019	GRAPH	1	0.0071				0.0405	1.0000	
10	1012	GRAPH	1	0.0010				0.0565	1.0000	
5	1006	GRAPH	1	0.0010				0.0565	1.0000	

VARIABLE FILM COEFF.

TABLE	TIME	COEFF	TIME	COEFF	TIME	COEFF	TIME	COEFF	TIME	COEFF

Table I (Continued)

SURFACE CONVECTORS

NODES		MECHANISM	WIDTH	DEPTH	AREA	FILM COEF
1001	2001	FORCE CONVEC	0.0140	1.0000	0.0001	3070.0000
1007	2001	FORCE CONVEC	0.0140	1.0000	0.0001	3070.0000
1013	2001	FORCE CONVEC	0.0140	1.0000	0.0001	3070.0000
1020	2001	FORCE CONVEC	0.0140	1.0000	0.0001	3070.0000
1026	2001	FORCE CONVEC	0.0140	1.0000	0.0001	3070.0000
1032	2001	FORCE CONVEC	0.0140	1.0000	0.0001	3070.0000
1038	2003	FORCE CONVEC	0.0140	1.0000	0.0001	3070.0000
1043	2003	FORCE CONVEC	0.0140	1.0000	0.0001	3070.0000
1049	2003	FORCE CONVEC	0.0140	1.0000	0.0001	3070.0000
1055	2003	FORCE CONVEC	0.0140	1.0000	0.0001	3070.0000
1061	2003	FORCE CONVEC	0.0140	1.0000	0.0001	3070.0000
1067	2003	FORCE CONVEC	0.0140	1.0000	0.0001	3070.0000
1073	2004	FORCE CONVEC	0.0140	1.0000	0.0001	3070.0000
1078	2005	FORCE CONVEC	0.0140	1.0000	0.0001	3070.0000
1084	2005	FORCE CONVEC	0.0140	1.0000	0.0001	3070.0000
1091	2005	FORCE CONVEC	0.0140	1.0000	0.0001	3070.0000
1096	2005	FORCE CONVEC	0.0140	1.0000	0.0001	3070.0000
1101	2005	FORCE CONVEC	0.0140	1.0000	0.0001	3070.0000
1106	2005	FORCE CONVEC	0.0140	1.0000	0.0001	3070.0000
1083	2002	RADIATION	0.0375	1.0000	0.0004	151.8075
1090	2002	RADIATION	0.0405	1.0000	0.0003	151.8075
1019	2002	RADIATION	0.0405	1.0000	0.0003	151.8075
1012	2002	RADIATION	0.0375	1.0000	0.0004	151.8075
1006	2002	RADIATION	0.0375	1.0000	0.0004	151.8075

INITIAL INTERNAL TEMPERATURES

NODE	TEMP	NODE	TEMP	NODE	TEMP	NODE	TEMP	NODE	TEMP
1	4500.00	2	4500.00	3	4500.00	4	4500.00	5	4500.00
6	4500.00	7	4500.00	8	4500.00	9	4500.00	10	4500.00
11	4500.00	12	4500.00	13	4500.00	14	4500.00	15	4500.00
16	4500.00	17	4500.00	18	4500.00	19	4500.00	20	4500.00
21	4500.00	22	4500.00	23	4500.00	24	4500.00	25	4500.00
26	4500.00	27	4500.00	28	4500.00	29	4500.00	30	4500.00
31	4500.00	32	4500.00	33	4500.00	34	4500.00	35	4500.00
36	4500.00	37	4500.00	38	4500.00	39	4500.00	40	4500.00
41	4500.00	42	4500.00	43	4500.00	44	4500.00	45	4500.00
46	4500.00	47	4500.00	48	4500.00	49	4500.00	50	4500.00
51	4500.00	52	4500.00	53	4500.00	54	4500.00	55	4500.00
56	4500.00	57	4500.00	58	4500.00	59	4500.00	60	4500.00
61	4500.00	62	4500.00	63	4500.00	64	4500.00	65	4500.00
66	4500.00	67	4500.00	68	4500.00	69	4500.00	70	4500.00
71	4500.00	72	4500.00	73	4500.00	74	4500.00	75	4500.00
76	4500.00	77	4500.00	78	4500.00	79	4500.00	80	4500.00
81	4500.00	82	4500.00	83	4500.00	84	4500.00	85	4500.00
86	4500.00	87	4500.00	88	4500.00	89	4500.00	90	4500.00
91	4500.00	92	4500.00		4500.00	94	4500.00	95	4500.00
96	4500.00	97	4500.00						

Astronuclear Laboratory
WANL-TME-1558

Table II

Typical Program Printouts
Ohmic Heating With Heat Generation in NbC, 850 KW Total Power

INTERNAL TEMPERATURES

NODE	TEMP	NODE	TEMP	NODE	TEMP	NODE	TEMP	NODE	TEMP
1	4880.70	2	4894.11	3	4915.48	4	4918.52	5	4906.43
6	4942.90	7	4958.27	8	4983.66	9	4997.01	10	4990.07
11	5034.42	12	5052.82	13	5084.07	14	5113.08	15	5118.42
16	5112.60	17	5104.32	18	5124.93	19	5160.21	20	5195.02
21	5205.73	22	5146.60	23	5168.57	24	5206.28	25	5243.14
26	5255.14	27	5166.70	28	5189.23	29	5227.93	30	5265.53
31	5277.96	32	5294.23	33	5320.55	34	5365.38	35	5408.11
36	5423.12	37	5294.27	38	5320.59	39	5365.90	40	5408.13
41	5423.14	42	5294.29	43	5320.60	44	5365.91	45	5408.15
46	5423.15	47	5294.28	48	5320.60	49	5365.91	50	5408.15
51	5423.15	52	5294.36	53	5320.66	54	5365.94	55	5408.16
56	5423.16	57	5294.18	58	5320.50	59	5365.84	60	5408.08
61	5423.09	62	5294.95	63	5321.27	64	5366.59	65	5408.83
66	5423.84	67	5011.17	68	5028.57	69	5057.26	70	5068.91
71	5059.56	72	5073.46	73	5092.96	74	5126.00	75	5153.50
76	5155.50	77	5141.70	78	5135.97	79	5157.61	80	5194.68
81	5230.35	82	5241.38	83	5179.36	84	5202.28	85	5241.62
86	5279.59	87	5292.19	88	5204.99	89	5228.69	90	5269.45
91	5308.48	92	5321.70	93	5217.46	94	5241.44	95	5282.68
96	5322.08	97	5335.52						

SURFACE TEMPERATURES

NODE	TEMP	CONNECT	FILM COEF	SURFACE FLUX	CONNECT	FILM COEF	SURFACE FLUX
1001	4873.27						
		2001	3070.000	0.1453E 07			
1002	0.						
1003	0.						
1004	0.						
1005	0.						
1006	4904.82						
		2002	180.830	0.3444E 06			
1007	4934.56						
		2001	3070.000	0.1641E 07			
1008	0.						
1009	0.						
1010	0.						
1011	0.						

Astronuclear Laboratory
WANL-TME-1558

Table II (Continued)

1012	4988.23		
		2002	187.294 0.3724E 06
1013	5024.68		
		2001	3070.000 0.1918E 07
1014	0.		
1015	0.		
1016	0.		
1017	0.		
1018	0.		
1019	5098.55		
		2002	196.122 0.4116E 06
1020	5094.51		
		2001	3070.000 0.2129E 07
1021	0.		
1022	0.		
1023	0.		
1024	0.		
1025	0.		
1026	5135.10		
		2001	3070.000 0.2257E 07
1027	0.		
1028	0.		
1029	0.		
1030	0.		
1031	0.		
1032	5154.90		
		2001	3070.000 0.2318E 07
1033	0.		
1034	0.		
1035	0.		
1036	0.		
1037	0.		
1038	5280.49		
		2003	3070.000 0.2703E 07
1039	0.		
1040	0.		
1041	0.		
1042	0.		
1043	5281.53		
		2003	3070.000 0.2703E 07
1044	0.		
1045	0.		
1046	0.		
1047	0.		
1048	0.		
1049	5280.55		
		2003	3070.000 0.2703E 07

Astronuclear Laboratory
WANL-TME-1558

Table II (Continued)

1050	0.		
1051	0.		
1052	0.		
1053	0.		
1054	0.		
1055	5280.54		
		2003	3070.000 0.2703E 07
1056	0.		
1057	0.		
1058	0.		
1059	0.		
1060	0.		
1061	5280.63		
		2003	3070.000 0.2704E 07
1062	0.		
1063	0.		
1064	0.		
1065	0.		
1066	0.		
1067	5280.44		
		2003	3070.000 0.2703E 07
1068	0.		
1069	0.		
1070	0.		
1071	0.		
1072	0.		
1073	5281.20		
		2004	3070.000 0.2705E 07
1074	0.		
1075	0.		
1076	0.		
1077	0.		
1078	5061.74		
		2005	3070.000 0.1847E 07
1079	0.		
1080	0.		
1081	0.		
1082	0.		
1083	5057.65		
		2002	192.813 0.3967E 06
1084	5063.12		
		2005	3070.000 0.2036E 07
1085	0.		
1086	0.		
1087	0.		
1088	0.		
1089	0.		

Astronuclear Laboratory
WANL-TME-1558

Table II (Continued)

090	5127.25			
		2002	198.464	0.4222E 06
1091	5124.64			
		2005	3070.000	0.2225E 07
1092	0.			
1093	0.			
1094	0.			
1095	0.			
1096	5167.37			
		2005	3070.000	0.2356E 07
1097	0.			
1098	0.			
1099	0.			
1100	0.			
1101	5192.61			
		2005	3070.000	0.2433E 07
1102	0.			
1103	0.			
1104	0.			
1105	0.			
1106	5204.92			
		2005	3070.000	0.2471E 07
1107	0.			
1108	0.			
1109	0.			
1110	0.			

BOUNDARY TEMPERATURES

NODE	TEMP	NODE	TEMP	NODE	TEMP	NODE	TEMP	NODE	TEMP
2001	4400.00	2002	3000.00	2003	4400.00	2004	4400.00	2005	4400.00

RATE OF TEMPERATURE CHANGE

NODE	RATE	NODE	RATE	NODE	RATE	NODE	RATE	NODE	RATE
1	0.	2	0.	3	0.	4	0.	5	0.
6	0.	7	0.	8	0.	9	0.	10	0.
11	0.	12	0.	13	0.	14	0.	15	0.
16	0.	17	0.	18	0.	19	0.	20	0.
21	0.	22	0.	23	0.	24	0.	25	0.
26	0.	27	0.	28	0.	29	0.	30	0.
31	0.	32	0.	33	0.	34	0.	35	0.
36	0.	37	0.	38	0.	39	0.	40	0.
41	0.	42	0.	43	0.	44	0.	45	0.
46	0.	47	0.	48	0.	49	0.	50	0.
51	0.	52	0.	53	0.	54	0.	55	0.
56	0.	57	0.	58	0.	59	0.	60	0.
61	0.	62	0.	63	0.	64	0.	65	0.
66	0.	67	0.	68	0.	69	0.	70	0.

Astronuclear Laboratory
WANL-TME-1558

Table II (Continued)

71	0.	72	0.		0.	74	0.	75	0.
76	0.	77	0.	78	0.	79	0.	80	0.
81	0.	82	0.	83	0.	84	0.	85	0.
86	0.	87	0.	88	0.	89	0.	90	0.
91	0.	92	0.	93	0.	94	0.	95	0.
96	0.	97	0.						

THE TEMPERATURE DISTRIBUTION HAS REACHED A STEADY STATE CONDITION

TABLE III

DISTRIBUTION OF NODES AMONG THE 9 HEAT GENERATION BANDS

BAND NO.	NODE NO.	HEAT GENERATION RATE, $Btu/In^3-Hr.$
1	4 5 9 10 15 16 70 71 76 77	3.4×10^5
2	1 2 3 6 7 8 13 14 69 74 75	2.4×10^5
3	17 18 19 20 21 80 81 82	1.8×10^5
4	22 23 24 25 26 85 86 87	1.4×10^5

TABLE III (Continued)

BAND NO.	NODE NO.	HEAT GENERATION RATE, $Btu/In^3-Hr.$
5	27	1.0×10^5
	28	
	29	
	30	
	31	
	90	
	91	
	92	
	95	
	96	
6	35	0.8×10^5
	36	
	40	
	41	
	97	
7	32	0.6×10^5
	33	
	34	
	37	
	38	
	39	
	42	
	43	
	44	
	45	
	46	
8	47	0.4×10^5
	48	
	49	
	50	
	51	
	52	
	53	
	54	
	55	
	56	
	57	
	58	
	59	

TABLE III (Continued)

BAND NO.	NODE NO.	HEAT GENERATION RATE, $Btu/In^3 - Hr.$
9	60	0.3×10^5
	61	
	62	
	63	
	64	
	65	
	66	